

X-553-72-50

PREPRINT

NASA TM X- 66012

# PRELIMINARY STUDY OF THE APPLICATION OF THE TIMATION III SATELLITE TO EARTH PHYSICS

Edited by  
**LLOYD CARPENTER**

(NASA-TM-X-66012) PRELIMINARY STUDY OF THE  
APPLICATION OF THE TIMATION 3 SATELLITE TO  
EARTH PHYSICS L. Carpenter (NASA) Mar.  
1972 25 p

N72-32851

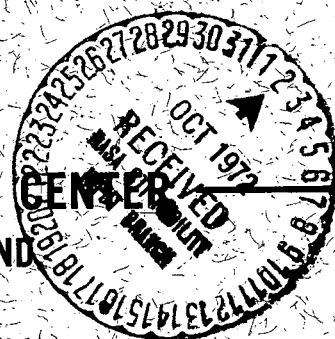
CSCL 22C

G3/31 Unclass  
41753

**MARCH 1972**



**GODDARD SPACE FLIGHT CENTER**  
**GREENBELT, MARYLAND**



Reproduced by  
**NATIONAL TECHNICAL  
INFORMATION SERVICE**  
U S Department of Commerce  
Springfield VA 22151

PRELIMINARY STUDY OF THE APPLICATION  
OF THE TIMATION III SATELLITE  
TO EARTH PHYSICS

Edited by  
Lloyd Carpenter

March 1972

Geodynamics Branch  
GODDARD SPACE FLIGHT CENTER  
Greenbelt, Maryland 20771

PRECEDING PAGE BLANK NOT FILMED

PRELIMINARY STUDY OF THE APPLICATION  
OF THE TIMATION III SATELLITE  
TO EARTH PHYSICS

ABSTRACT

An important aspect of the earth physics program is the utilization of accurate (10 cm) laser ranging observations of artificial satellites to determine significant geodynamic parameters such as polar motion, sea floor spreading, solid earth tides, and earth rotation. The successful accomplishment of these objectives depends on the judicious selection of satellites to be fitted with laser reflectors. A promising candidate is TIMATION III, which is a U. S. Navy timing and navigation satellite originally planned for launch in December 1972 into a circular orbit at  $98^\circ$  inclination and 14,000 km altitude with gravity gradient stabilization. With this configuration the usually troublesome effects of drag and higher order geopotential terms are minimized. An error analysis indicates a satellite position uncertainty of about one meter, 80% of which is attributable to the assumed gravity model errors. The remaining uncertainties have a period equal to that of the satellite and can be filtered out yielding an effective uncertainty of about 10 cm in the study of phenomena having different periodicities. The accomplishment of these results depends on a careful consideration of solar radiation pressure taking account of the spacecraft reflecting properties and variations in the presentation area. Consideration is also given to the displacement of the laser reflectors from the center of mass of the spacecraft and to the dynamic coupling of any libration in attitude with the orbital motion. The results indicate that a good set of well distributed laser observations of TIMATION III could yield determinations of polar motion, sea floor spreading, solid earth tides, and earth rotation at the 10 cm level. The planned launch date and orbital parameters were modified after this study was made. However, it is felt that the conclusions remain essentially valid, and the results will be of interest in planning similar missions.

Preceding page blank

	<u>Page</u>
INTRODUCTION.....	1
ORBITAL PERTURBATIONS.....	5
ERROR ANALYSIS.....	13
COUPLING BETWEEN SPACECRAFT DYNAMICS AND ORBITAL MOTIONS .....	17
CONCLUSIONS .....	21
ACKNOWLEDGMENT .....	21
References .....	21

Preceding page blank

# PRELIMINARY STUDY OF THE APPLICATION OF THE TIMATION III SATELLITE TO EARTH PHYSICS

## INTRODUCTION

TIMATION III is a U.S. Navy timing and navigation satellite planned for launch in December 1972. The spacecraft will have the shape of a hollow, twelve-sided cylinder of approximately 132 cm outside diameter, 51 cm inside diameter, and 71 cm length. It will weigh approximately 160 kg and will be gravity gradient stabilized (by a ball on the end of a boom parallel to the axis of the cylinder). Cube corner retroreflectors will be placed around the base of the cylinder for laser ranging.

The nominal orbit will be circular and near polar ( $98^\circ$  inclination) at an altitude of 14,000 km having an 8-hour orbital period. TIMATION III is especially well suited to earth physics studies because the spacecraft design and orbit configuration facilitate precise measurements in which the effects of poorly determined modeling parameters are minimized while the signature of the properties under study is enhanced. The cube corner retroreflectors on the end of the cylindrical shape should give a sharp return signal. With the gravity gradient stabilization, it should be possible to relate the center of the reflecting area to the center of mass of the satellite to an accuracy of about 10 cm, determined largely by the quality of the stabilization. The troublesome effects of drag and high degree and order harmonics in the earth's potential are not expected to be a problem at the 14,000 km altitude. The accurate computation of radiation pressure will be important, and it will be necessary to account for the complex shape of the spacecraft and the known orientation, while the troublesome shadow effects will be absent over periods of several months due to the high inclination of the orbit and its high altitude. The radiation pressure perturbations may be the limiting factor in the reduction of the residuals as is discussed later in this report.

If the spherical earth approximation is used, the range,  $\rho$ , and elevation,  $\ell$ , from an observing station are functions only of the geocentric separation angle,  $\psi$ , for a circular orbit of given radius,  $r$  (see Figure 1). If, in addition, the satellite is gravity gradient stabilized, the angle  $\epsilon$  between the geocentric position vector (or spin axis) and the line of sight from the station depends only on  $\psi$ . Letting  $r_e$  be the radius of the earth,

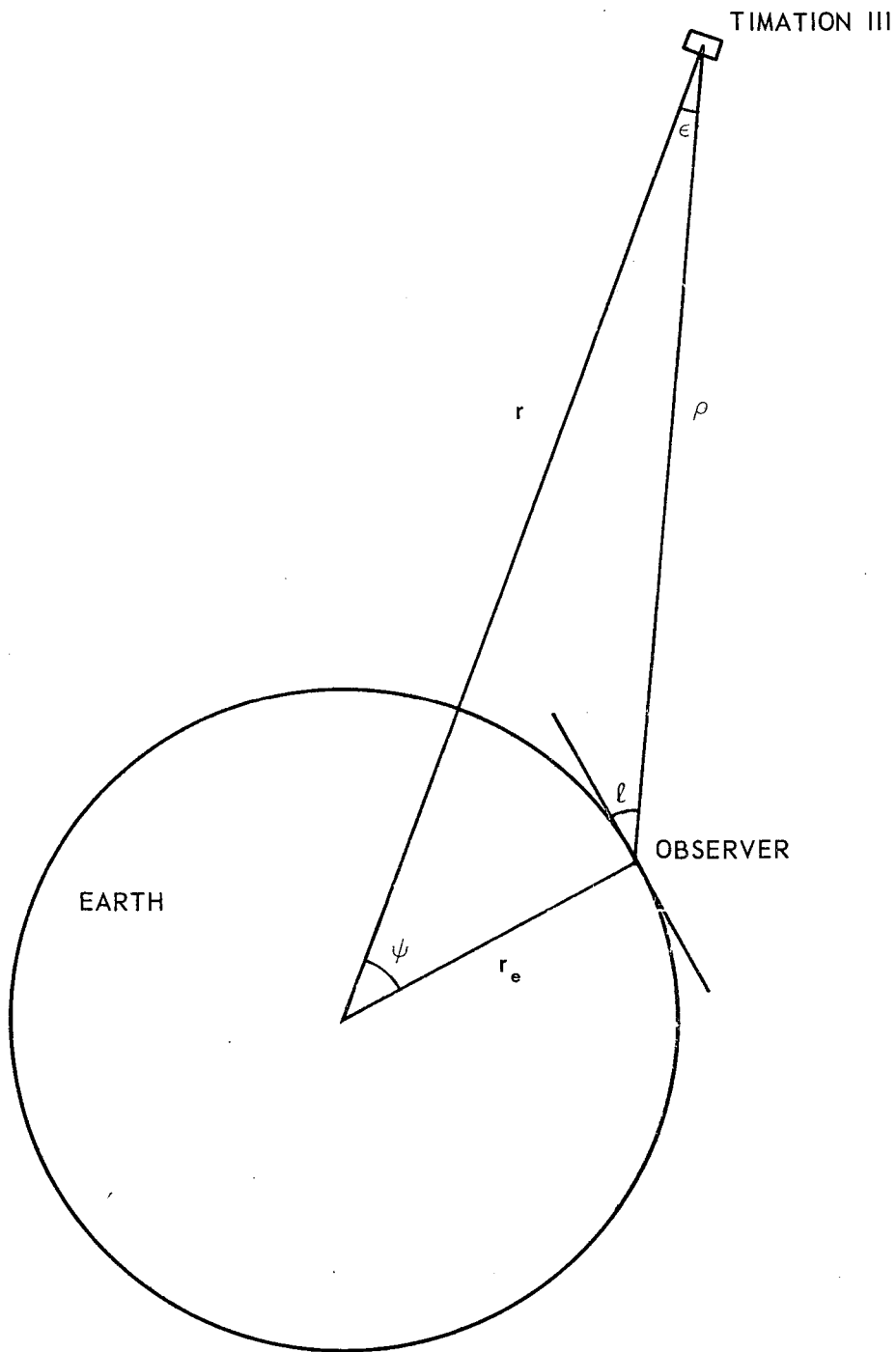


Figure 1. Range and Elevation Geometry for TIMATION III

$$\rho^2 = r_e^2 + r^2 - 2 r r_e \cos \psi$$

$$\sin \ell = \frac{r}{\rho} \cos \psi - \frac{r_e}{\rho} \quad -90^\circ \leq \ell \leq 90^\circ$$

$$\sin \epsilon = \frac{r_e}{\rho} \sin \psi \quad 0 \leq \epsilon < 90^\circ.$$

The values are plotted in Figure 2 for the assumed altitude of 14,000 km. The angle  $\epsilon$  between the spin axis and the line of sight remains less than  $20^\circ$  so that the station is always looking at the base of the spacecraft. The angle  $\epsilon$  must be known in order to correct the measured range for the displacement of the cube corners from the center of mass. More importantly, we see that the elevation is above  $12^\circ$  whenever the geocentric angle between the station and the spacecraft does not exceed  $60^\circ$ . If the satellite were directly over the North Pole at this altitude, its elevation from Goddard would be  $22^\circ$  and its range 17,100 km. Because of the  $98^\circ$  inclination, the actual elevation from Goddard would be between  $13^\circ$  and  $32^\circ$  each time the satellite reaches its maximum latitude. The corresponding range to the satellite would be between 18,000 and 16,300 km. Simultaneous laser ranging from Goddard and a station in Europe would provide precise determinations of polar motion. Corresponding measurements as the satellite passes over the Atlantic Ocean would provide a measure of sea-floor spreading and U.T. 1. Laser ranging to the satellite as it passes overhead would provide a direct measure of solid earth tides. The eight-hour period results in resonance with the (3,3) terms in the earth's potential. The accurate laser observations would improve the accuracy of these third order coefficients by an order of magnitude as well as improving the value of GM by two orders of magnitude.

The geocentric separation,  $\psi$ , can be removed from the relationships giving, for example,

$$\sin \ell = \frac{r^2 - r_e^2 - \rho^2}{2 \rho r_e}$$

$$\cos \epsilon = \frac{r^2 - r_e^2 + \rho^2}{2 \rho r}$$

$$\rho = -r_e \sin \ell + \sqrt{r^2 - r_e^2 \cos^2 \ell}$$

$$\sin \epsilon = \frac{r_e}{r} \cos \ell.$$

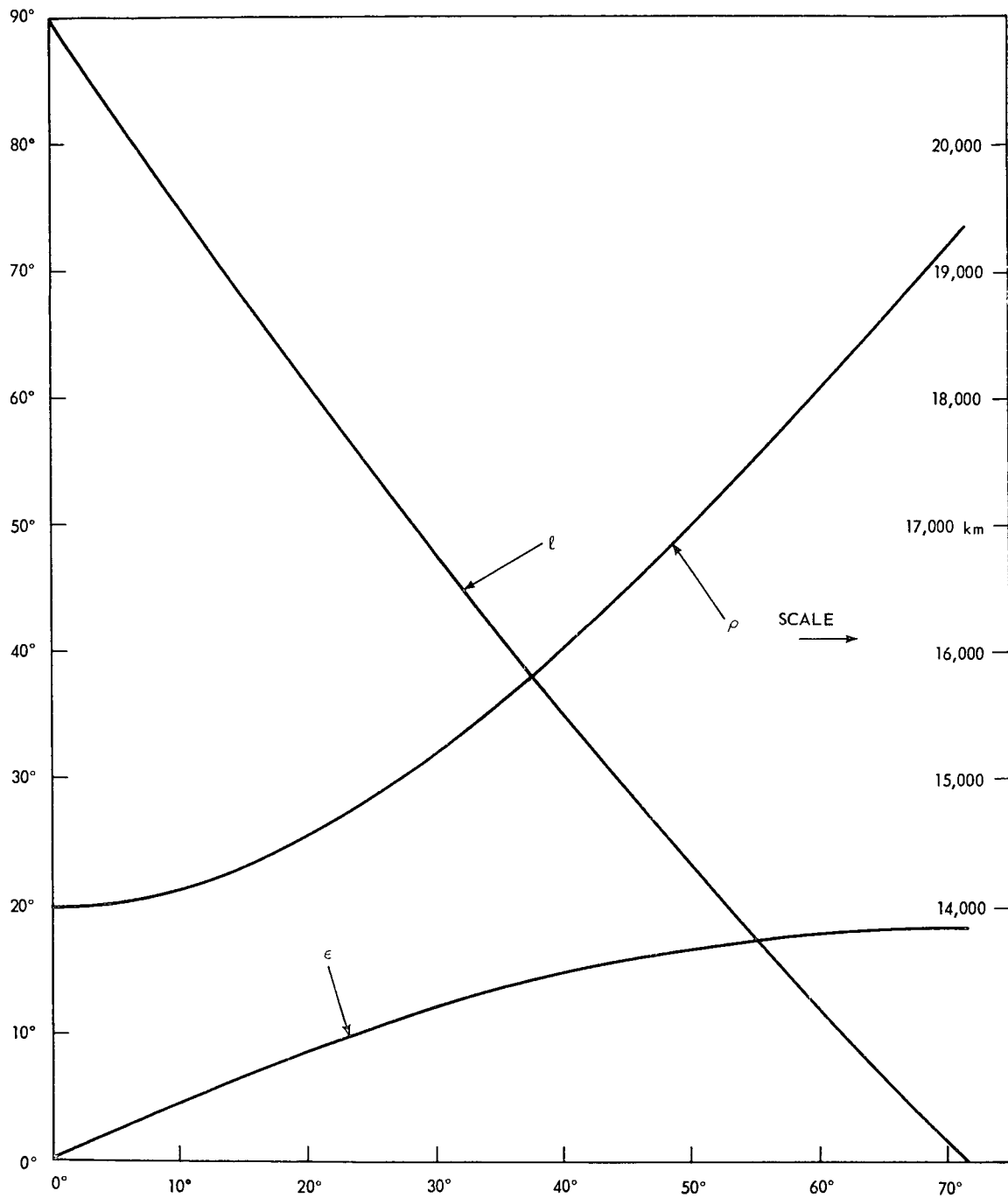


Figure 2. TIMATION III. Variation of the range,  $\rho$ , the elevation,  $\ell$ , and the angle  $\epsilon$  between the spin axis and the line of sight with the geocentric separation angle,  $\psi$ , between the observer and the satellite.



For convenience,  $\ell$  and  $\epsilon$  are plotted as functions of the range,  $\rho$ , in Figure 3.

To obtain the desired degree of accuracy in treating observations of TIMATION III, it will be necessary to consider effects which are usually neglected. The coupling of spacecraft dynamics to the orbital motion may fall into this category. This problem is discussed later in this report.

## ORBITAL PERTURBATIONS

The nominal orbit that was used in computing the perturbations was one with a semimajor axis of 3.195 earth radii, an eccentricity of .0025, and an inclination of  $98^\circ$ . The epoch was December 1, 1972 at  $0^h$ . The geopotential perturbations were computed using a subset of the SAO Standard Earth II. The coefficients used in the computations were limited for the most part to a group of low degree zonal and tesseral harmonics. An average presentation area to mass ratio of  $0.1 \text{ cm}^2/\text{gm}$  was used in computing perturbations due to solar radiation. The most significant secular, long-period, and intermediate period perturbations in the Keplerian elements due to the geopotential, lunar and solar gravity, and direct solar radiation are summarized in Tables 1 and 2. These tables give some indication of the relative effect of the different sources of the perturbations. These terms and all the others combine in different ways depending on the initial values of the argument of perigee,  $\omega$ , and longitude of the ascending node,  $\Omega$ .

The perturbations were computed for 300 days with various combinations of initial values of  $\omega$  and  $\Omega$ . The maximum variations in the elements were as follows:  $\Delta a = 4.6 \text{ km}$ ,  $\Delta e = 3.8 \times 10^{-4}$  or .15 e,  $\Delta I = 0^\circ 15'$ ,  $\Delta M = 21^\circ 9'$ ,  $\Delta \omega = 7^\circ 5'$ , and  $\Delta \Omega = 0^\circ 50'$ . (a, semi-major axis; e, eccentricity; I, orbital inclination; M, mean anomaly)

Certain components in the perturbations are of special interest since geodetic parameters may be recovered directly from a precise knowledge of the orbit. Included here would be improvement in our knowledge of the gravity field (especially low degree zonal and tesseral harmonics). The amplitude and period of the resonant perturbations are illustrated in Figure 4 which shows the evolution of the semi-major axis (see also Table 3).

The perturbations due to the solid earth tides, assuming a  $k_2$  Love number of .3 are too small to be used to improve  $k_2$  since they amount to only about  $''2$ ,  $''5$ , and  $2''7$  in inclination, longitude of the ascending node, and argument of latitude respectively in a one year period. Solid Earth tidal effects will, however, be discernable geometrically directly from the range measurements. Perturbations in the Keplerian elements due to precession and nutation are much larger (see

Table 1  
Principal Periodic Perturbations

Element	Force	Intermediate Period			Long Period		
		Amplitude	Argument	Period (days)	Amplitude	Argument	Period (days)
a	$J_{3,3}$	1600 m	$3M + 3\Omega - 3\theta_g$	42			
e	sun	$-1.4 \cdot 10^{-6}$	$2\lambda_{\odot} + 2\omega - 2\Omega$	203	$2.1 \cdot 10^{-5}$	$2\omega$	2333
e	moon	$1.5 \cdot 10^{-6}$	$3\lambda_{\text{♁}} + \Omega_{\text{♁}} - 3\Omega$	9	$4.1 \cdot 10^{-5}$	$2\omega$	2333
e	radiation*	$-4.7 \cdot 10^{-5}$	$\lambda_{\odot} + \omega - \Omega$	407			
I	sun	$1^{\circ}8 \cdot 10^{-2}$	$2\lambda_{\odot} - 2\Omega$	187	$0^{\circ}083$	$\Omega_{\odot} - \Omega$	15140
I	moon	$2^{\circ}8 \cdot 10^{-3}$	$2\lambda_{\text{♁}} - 2\Omega$	14	$0^{\circ}15$	$\Omega_{\text{♁}} - \Omega$	12345
I	radiation*	$5^{\circ}8 \cdot 10^{-6}$	$\lambda_{\odot} + \omega - \Omega$	407			
$\Omega$	sun	$7^{\circ}5 \cdot 10^{-3}$	$2\lambda_{\odot} - \Omega_{\odot} - \Omega$	185	$0^{\circ}24$	$2\Omega_{\odot} - 2\Omega$	7570
$\Omega$	moon	$1^{\circ}3 \cdot 10^{-3}$	$2\lambda_{\text{♁}} - \Omega_{\text{♁}} - \Omega$	14	$0^{\circ}40$	$2\Omega_{\text{♁}} - 2\Omega$	6173
$\Omega$	radiation*	$6^{\circ}3 \cdot 10^{-6}$	$\lambda_{\odot} + \omega - \Omega$	407			
$M + \omega$	sun	$3^{\circ}5 \cdot 10^{-2}$	$2\lambda_{\odot} - 2\Omega$	187	$0^{\circ}38$	$2\Omega_{\odot} - 2\Omega$	7570
$M + \omega$	moon	$4^{\circ}6 \cdot 10^{-3}$	$2\lambda_{\text{♁}} - 2\Omega$	14	$0^{\circ}69$	$2\Omega_{\text{♁}} - 2\Omega$	6173
$M + \omega$	radiation*	$8^{\circ}5 \cdot 10^{-6}$	$\lambda_{\odot} - \omega - \Omega$	346			

\*Direct solar radiation pressure

Notation: a semi-major axis  
e eccentricity  
I inclination

$\lambda$  mean longitude  
 $\Omega$  longitude of ascending node  
 $\omega$  argument of perigee

M mean anomaly  
 $\theta_g$  Greenwich sidereal time

$\text{♁}$  subscript for moon  
 $\odot$  subscript for sun

Table 2  
Secular Perturbations  
(degrees/day)

	Zonal	Lunar	Solar	Total
$\dot{\omega}$	-.07718	-.00094	-.00047	-.07859
$\dot{\Omega}$	.02380	.00029	.00014	.02423

Figures 5, 6, and 7). The perturbations amount to 12'', 3!5, and 4' in inclination, longitude of the ascending node, and argument of latitude in 660 days.

One of the main limiting factors in the determination of geodetic constants from this satellite orbit is the computation of solar radiation pressure perturbations. Although the radiation pressure effects are small relative to some of the other sources (see Table 1), the uncertainties in the computations of the effects are large due to several circumstances, such as: (1) the difficulty of accurately

Table 3

Principal Non-Zonal Along Track Effects	
Primary beat period is 41.6 days.	
(1)	Resonant terms: The (3,3) coefficients contribute terms with amplitude > 1000 m. The root-sum-square of resonant terms is 30260 m.
(2)	M-Daily terms: The (2,2) coefficients contribute longitude dependent terms with amplitude > 50 m. The following coefficients contribute terms > 1 m: (3,1), (4,1), (3,2), (4,2), (3,3), (4,4).
(3)	Short period terms: The following coefficients contribute mean anomaly dependent terms with amplitude > 1 m: (3,1), (3,2), (3,3), (4,4), (5,5).
The root-sum-square of non-resonant terms is 75 m.	

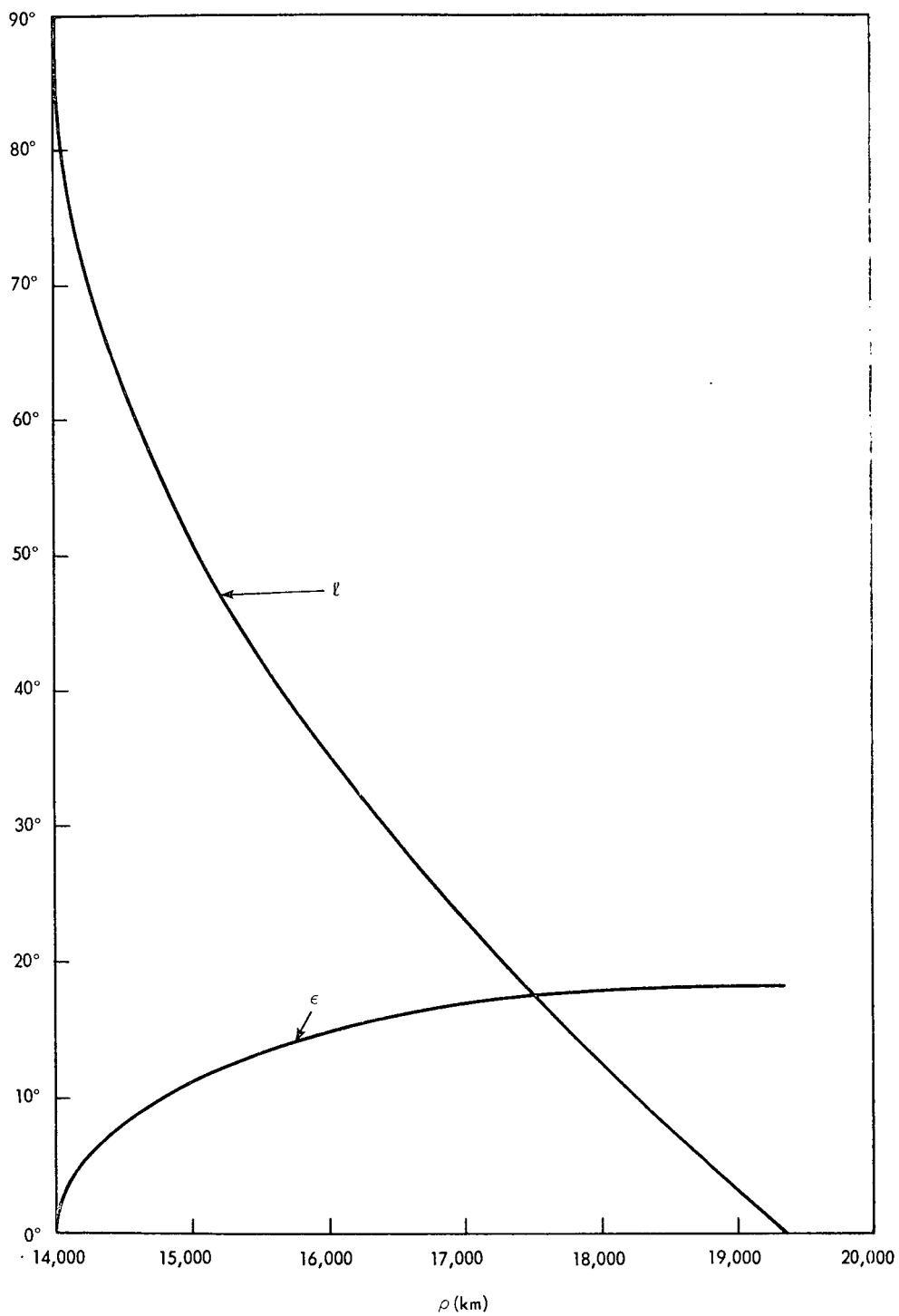


Figure 3. TIMATION III. Variation of the elevation,  $\ell$ , and the angle  $\epsilon$  between the spin axis and the line of sight with range,  $\rho$ .

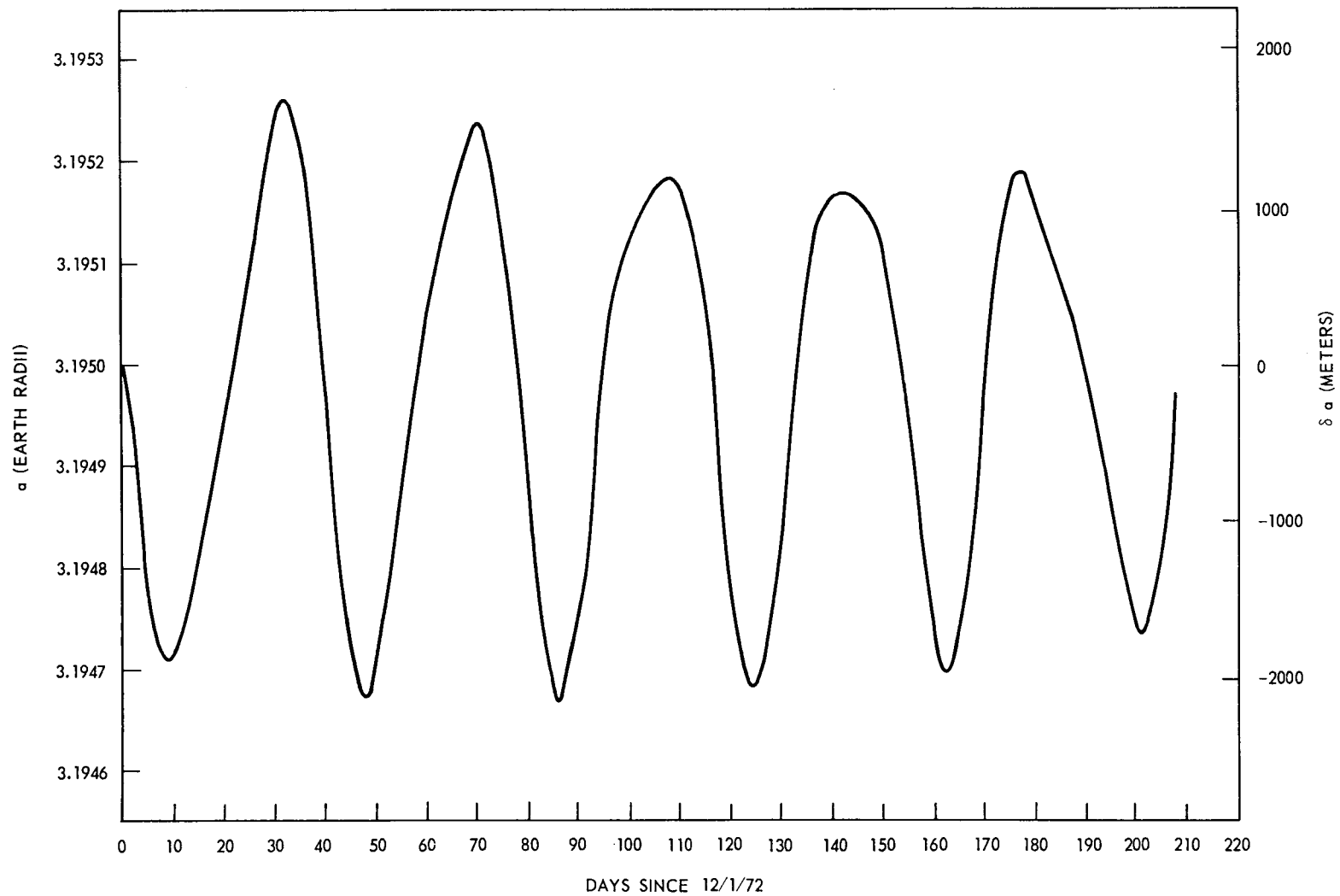


Figure 4. Resonant Geopotential Perturbations

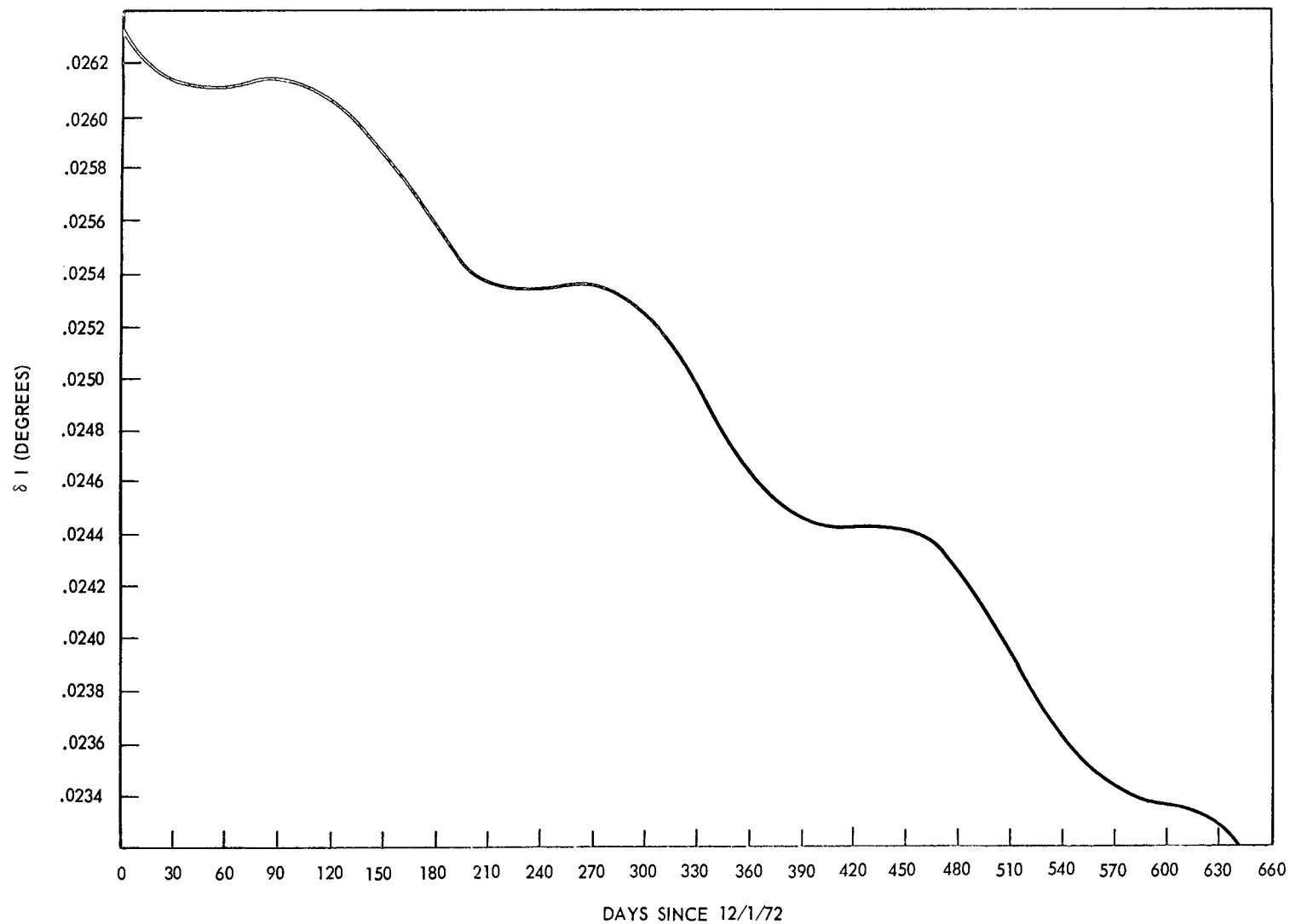


Figure 5. Precession and Nutation Perturbation

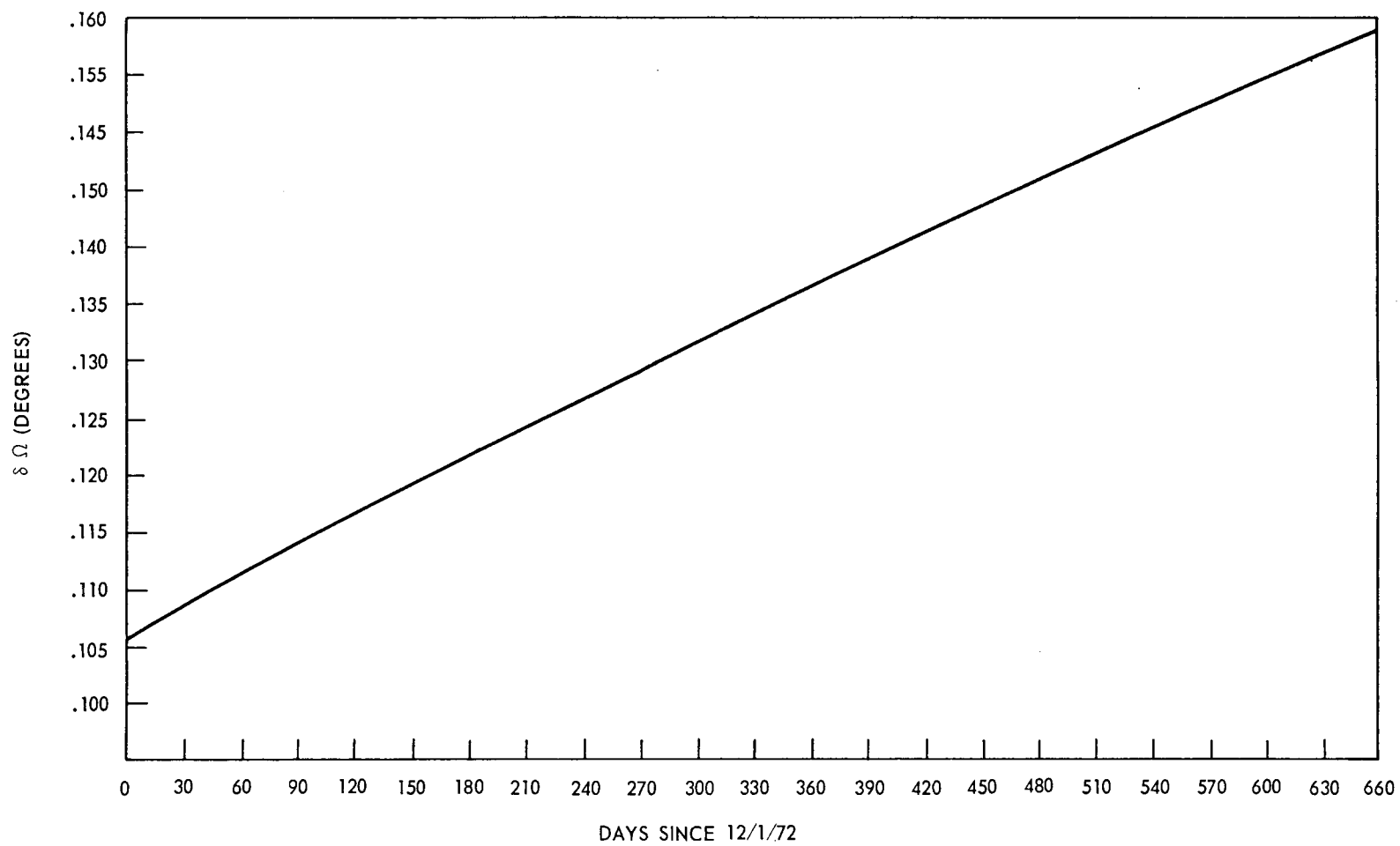


Figure 6. Precession and Nutation Perturbation

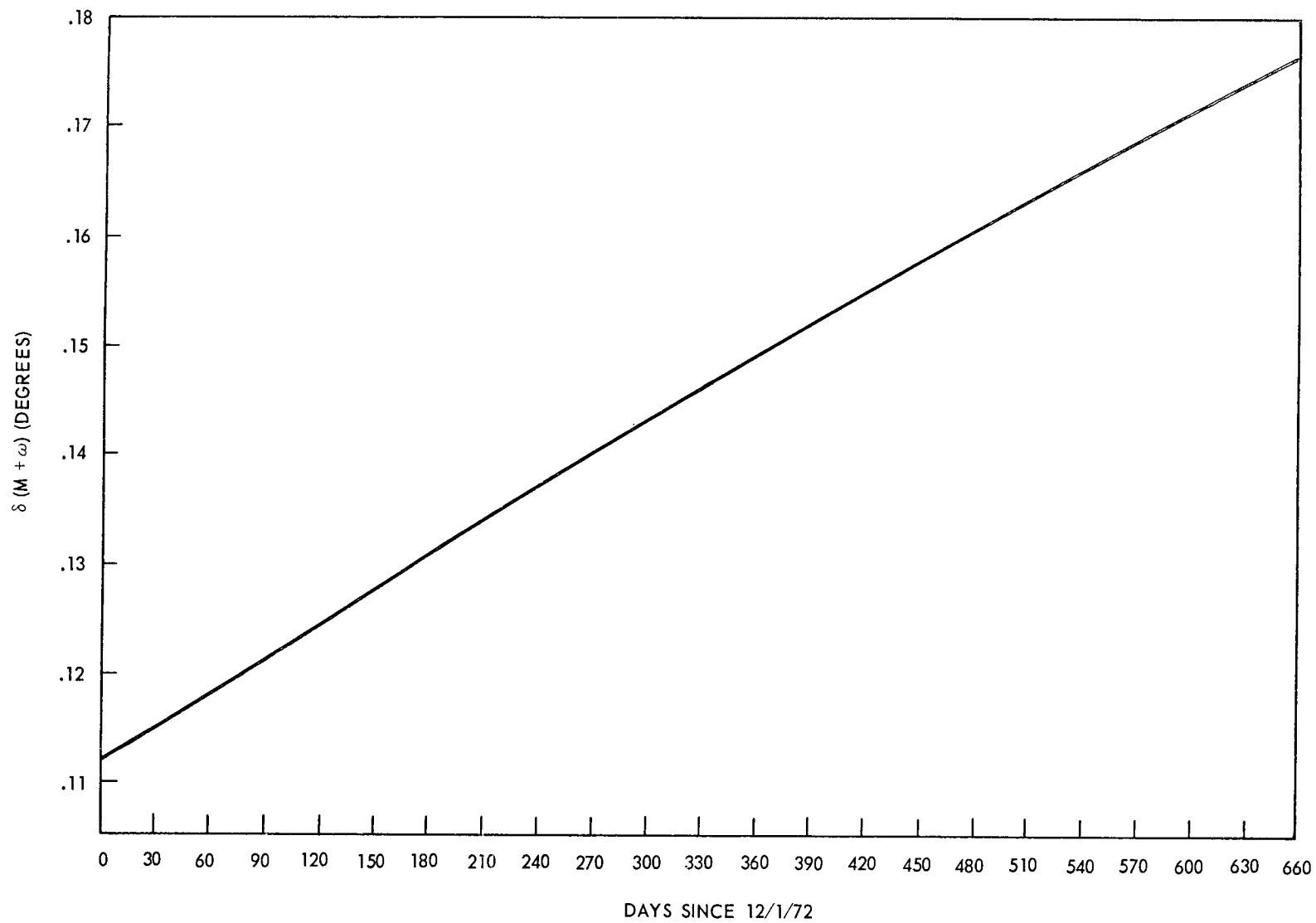


Figure 7. Precession and Nutation Perturbation



modeling the effect of solar radiation pressure in the penumbra region, (2) the effect of the earth's albedo, (3) the effect of a changing presentation area of the satellite to the sun, and (4) incomplete knowledge of the variable reflecting properties of the exposed surfaces. Sample computations indicate that a 10% error in the magnitude of the radiation pressure will produce a deviation in the computed position which oscillates and increases in amplitude reaching an amplitude of about 50 meters in the along track position after 10 days in complete sunlight. The shadow effect is about twice as large. This corresponds to a variation in the eccentricity which must be removed by accurately computing the radiation pressure, or by solving for this effect.

The neglect of the umbra-penumbra modeling causes an error that is bounded by the difference between considering the umbra and then the penumbra each as complete shadow. For TIMATION III this would amount to a difference of  $4^\circ$  in the application of the shadow. This in turn would amount to at most 11% of the shadow effect.

The albedo perturbations for near earth satellite orbits have been estimated to be about 5% of the direct effect. For TIMATION III this percentage will be less because the albedo perturbation varies inversely with  $a^2$ . Finally, the radiation force is affected by changes in the presentation area. For this satellite the ratio of maximum to minimum presentation area is about 1.6. An accurate presentation area could be computed simply from the knowledge that the spacecraft is gravity gradient stabilized.

Some conclusions concerning the radiation pressure can be made. Since it takes only one month out of every six for the earth's shadow moving at  $1^\circ/\text{day}$  to pass through the essentially fixed orbit, the geodetic experiments where possible should be conducted during periods of total sunlight. This would eliminate shadow related problems. Expressions for the albedo effect on the Keplerian elements could be applied as a part of the geodetic analysis. Allowance must be made for the varying presentation area of TIMATION III.

## ERROR ANALYSIS

This section contains a discussion of orbital error analysis simulations which have been performed. The existence of four laser tracking stations has been assumed for this study. The approximate locations of these stations are as follows:

<u>Station Name</u>	<u>Latitude</u>	<u>E. Longitude</u>
Winkfield, England	51°	359°
Greenbelt, Maryland	39°	283°
Naini Tal, India	29°	79°
Woomera, Australia	-31°	137°

Figure 8 indicates the orbital coverage provided by these stations for a period of two days. Several important points are demonstrated in this figure.

- Typical station pass lengths are on the order of two hours.
- Stations are able to observe the satellite on every revolution.
- Simultaneous tracking will be possible between most continents of the world.
- Continuous orbital coverage would be possible with five or more optimally located stations.

Using simulated range observations from these stations, an orbital solution was modeled for a seven day arc using standard techniques. The purpose of this simulation was to estimate the accuracy one could expect in solutions for orbital and geodetic parameters and to determine the effects of certain unmodeled tracking system and force model errors on the recovery of these parameters. In this simulation it was assumed that the orbit would be in 100% sunlight — a situation which occurs for several months at a time. Also since perturbations on the orbital elements of this satellite due to solar radiation pressure have a long period (i.e.  $\sim 1$  yr), it was assumed that the perturbation would appear secular over a period of seven days. Therefore a scale parameter was permitted to absorb any errors in modeling this perturbation.

The unmodeled errors assumed for the study were as follows:

<u>Error Source</u>	<u>Magnitude</u>
Earth Gravity Model	25% of the difference between the Applied Physics Laboratory -3.5 (1965) and the Smithsonian Astrophysical Observatory M-1 (1966) models up to degree and order 8.

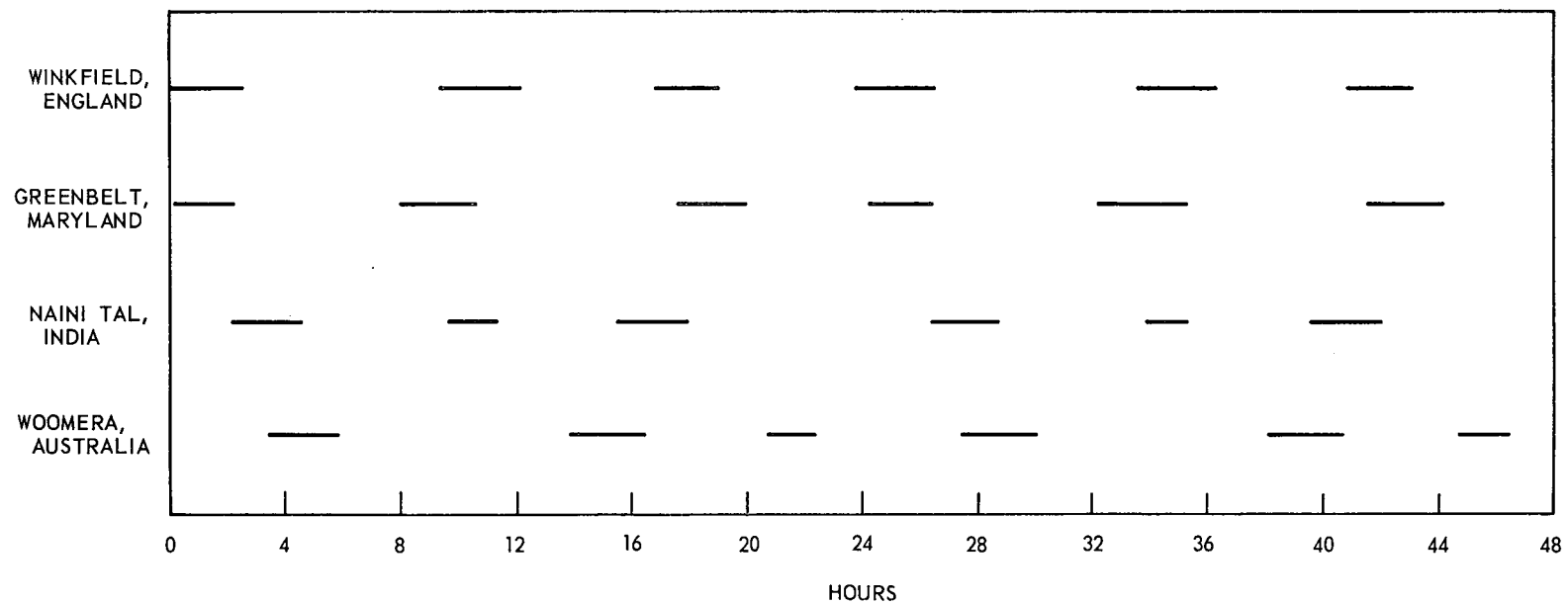


Figure 8. Orbital Coverage Provided By Laser Tracking Stations

<u>Error Source</u>	<u>Magnitude</u>
Laser range bias	10 cm
Laser range noise	10 cm

Naini Tal, India was taken as the origin of the system with no error in station position.

The table below presents the geodetic parameters adjusted in the 7 day orbital arc along with comments regarding the accuracy of the recovered values.

<u>Adjusted Parameter</u>	<u>Comments on Uncertainty of the Adjusted Value</u>
Gravity Coefficients C (3, 3) and S (3,3)	The orbit is in resonance with these third order coefficients. The uncertainty in the adjusted values would be reduced by about an order of magnitude with respect to the current state of the art.
GM	The uncertainty in GM would be reduced by two orders of magnitude (i.e. from $10^{-6}$ to $10^{-8}$ )
Winkfield Station Coordinates	Total uncertainty of adjusted coordinates $\sim 34$ cm.
Greenbelt Station Coordinates	Total uncertainty of adjusted coordinates $\sim 25$ cm.
Woomera Station Coordinates	Total uncertainty of adjusted coordinates $\sim 58$ cm.

In the recovery of C (3, 3) and S (3, 3) about 90% of the uncertainty arises from the errors in the other low degree and order gravity coefficients. This is also true in the recovery of GM where about 80% of the uncertainty can be attributed to the low degree and order gravity coefficients. The uncertainty of  $10^{-8}$  in the value of GM is commensurate with the computation of the orbital semi-major axis to an accuracy of about 10 cm and an uncertainty in the average along track motion of about 30 meters in seven days. In the case of the station coordinates the latitude and longitude uncertainties also are predominantly attributable to gravity model error. However the station height error is divided between tracking station bias and gravity model error. The recovery of the above parameters would be enhanced by perhaps a factor of five by utilizing multiple orbital arcs in a simultaneous solution.

Figure 9 presents a plot of the orbit uncertainties for the first two days of the seven day arc due to the unmodeled errors discussed earlier. The total position uncertainty has been resolved into three components, i.e. radial, cross track and along track. The along track uncertainties are generally under 1.5 meters with occasional excursions to about 3 meters. Cross track uncertainties are generally less than 1.2 meters and the uncertainty in the radial component seldom exceeds .75 meters.

In general about 80% of the satellite position uncertainty could be attributed to the assumed gravity model errors. These errors could, of course, be reduced by adjusting the values of the coefficients or obtaining improved values from another source. It is important to note, however, that the orbital uncertainties contain primarily a period corresponding to the orbital period of the satellite. The noise about the curves is only a few centimeters. Therefore in studying phenomena having a periodicity different from that of the orbit, one could filter out the effects having a period equal to the orbital period.

#### COUPLING BETWEEN THE SPACECRAFT DYNAMICS AND ORBITAL MOTIONS

A mathematical model of the interaction between the spacecraft dynamics and orbital motions for TIMATION III is described and the dynamical equations of motion are derived. The nonlinear coupled equations describing the behavior of the perturbed system in a neighborhood of assumed equilibrium solution have periodic terms. The results indicate that the variation in the radius vector has an amplitude of the order of 150 cm which is within the range of laser measurements.

The coupling between spacecraft dynamics and orbital motions is governed by three nonlinear second order differential equations (see Schindler 1959-1960)

$$\ddot{r} - r \dot{\theta}^2 + \frac{K}{r^2} = 0 \quad (1)$$

$$\ddot{\theta} + \ddot{\phi} + 3 \frac{K}{r^3} \cdot \frac{B-A}{C} \phi = 0 \quad (2)$$

$$r^2 \ddot{\theta} + 2 r \dot{r} \dot{\theta} + \frac{B}{M} (\ddot{\theta} + \ddot{\phi}) = 0 \quad (3)$$

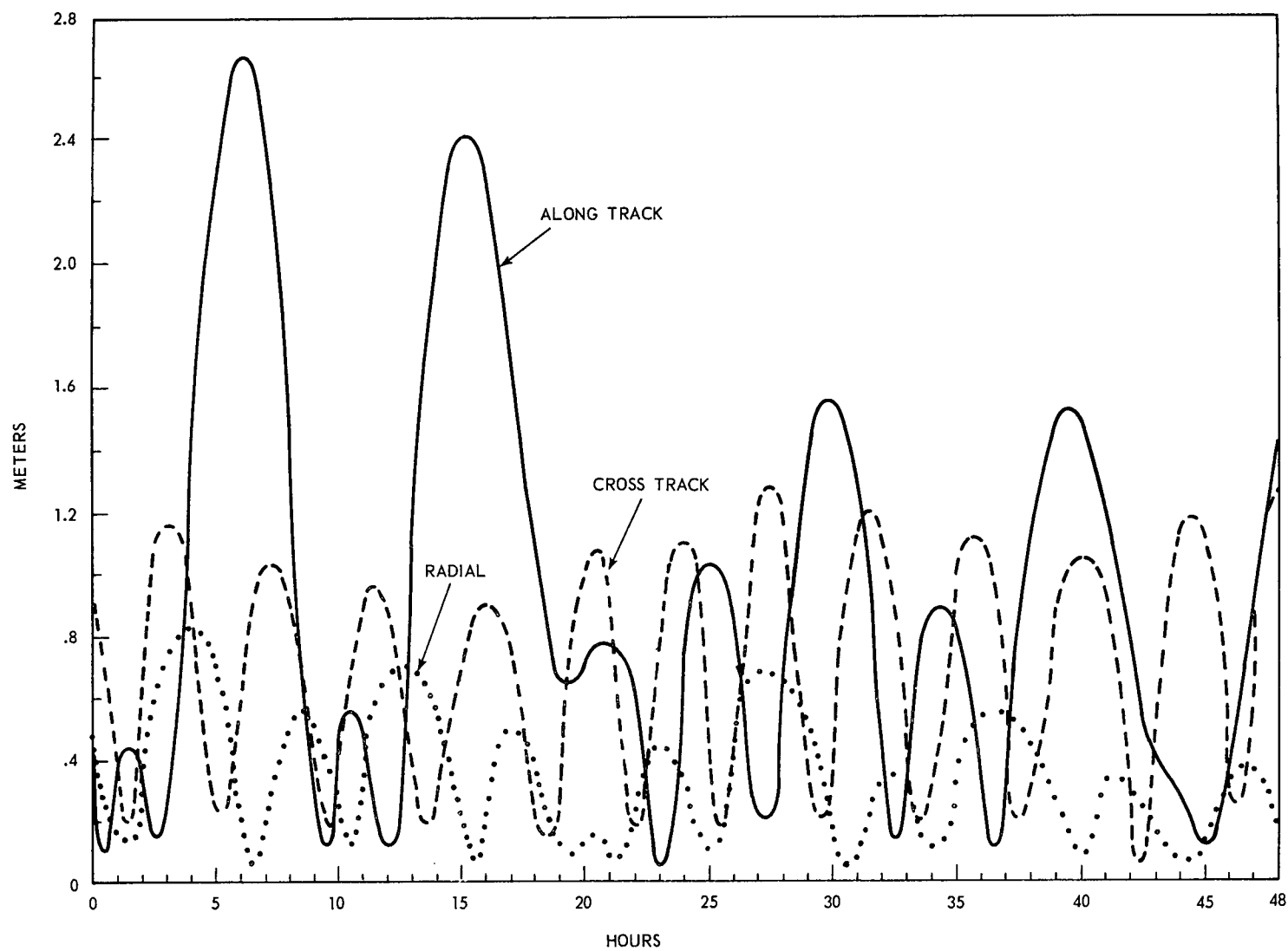


Figure 9. TIMATION III Orbital Uncertainty

where  $K$  is the gravitational parameter,  $r$  the radius from the satellite's center of mass to the center of the Earth,  $\theta$  the true anomaly,  $\phi$  the angle of libration in the orbit plane,  $M$  the mass of the satellite and  $A$ ,  $B$  and  $C$  are the principal, central moments of inertia of the satellite (see Figure 10).

Any effort to achieve the solution of the motion of the satellite must contend with the complications inherent in Equations (1), (2) and (3). An attempt to discuss the coupled motions has been made by using Hamiltonian perturbation techniques

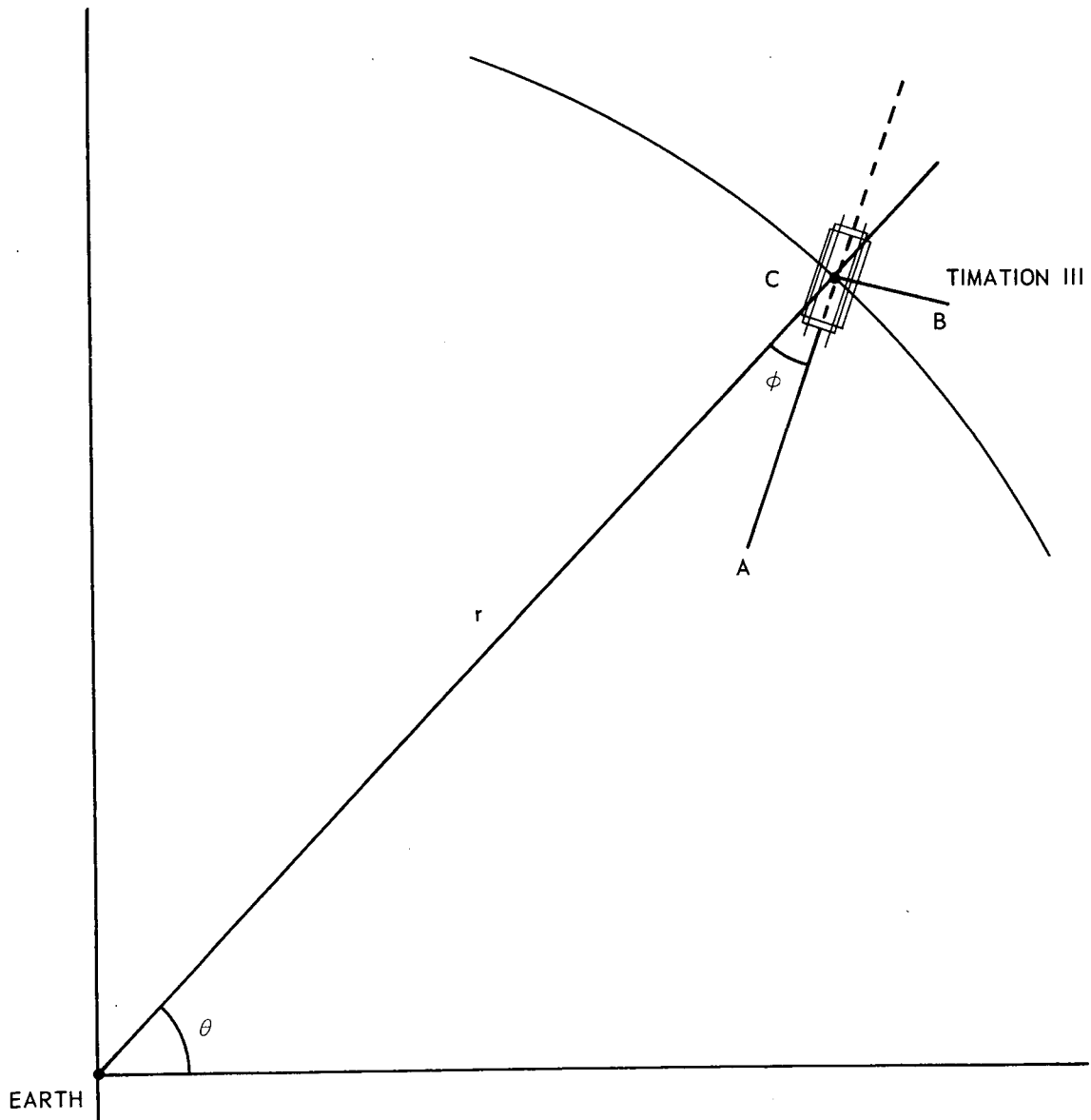


Figure 10

and iteration methods. The solutions of Equations (1), (2) and (3) are

$$\begin{aligned}
r = & r_0 + \frac{\dot{r}_0}{\omega_0} \left(1 - \frac{\ell}{r_0}\right) \left(1 + \frac{3}{2} \frac{\ell^2}{r_0^2}\right) \sin \omega_0 t \\
& + \frac{3}{2} \frac{\dot{r}_0^2}{r_0 \omega_0^2} \left(1 - \frac{\ell}{r_0}\right) \sin^2 \omega_0 t + \frac{5}{2} \frac{\dot{r}_0^3}{r_0^2 \omega_0^3} \sin^3 \omega_0 t \\
& + \frac{\sqrt{3}}{2} \cdot \frac{\ell^2}{r_0} \left(1 + \frac{\dot{r}_0 \sin \omega_0 t}{r_0 \omega_0}\right) \left[\phi_0 - \frac{\dot{r}_0}{r_0 \omega_0} \left(1 - \frac{\ell}{r_0}\right)\right] \sin \sqrt{3} \omega_0 t. \quad (4)
\end{aligned}$$

$$\theta = \omega_0 t + 2 \frac{\dot{r}_0^2}{r_0 \omega_0} \left(1 - \frac{\ell}{r_0}\right) (\cos \omega_0 t - 1) + \theta_0 \quad (5)$$

$$\phi = \frac{\dot{r}_0}{r_0 \omega_0} \left(1 - \frac{\ell}{r_0}\right) \cos \omega_0 t + \left[\phi_0 - \frac{\dot{r}_0}{r_0 \omega_0} \left(1 - \frac{\ell}{r_0}\right)\right] \cos \sqrt{3} \omega_0 t \quad (6)$$

where  $\ell = \sqrt{B/M}$ ,  $\omega_0 = \sqrt{K/r_0^3} = \dot{\theta}_0$  and  $r_0$ ,  $\dot{\theta}_0$  and  $\phi_0$  are initial constants.

To the order of approximation involved, the initial constants are coupled by

$$\phi_0 = \frac{2}{3} \frac{\dot{r}_0}{\ell \omega_0} \quad (7)$$

Equations (4), (5) and (6) are shown to have periodic terms. They describe the behavior of the perturbed satellite in a neighborhood of assumed equilibrium solution. If one adopts as representative values  $\ell = 5 \times 10^2$  cm,  $\phi_0 = 2 \times 10^{-1}$  (rad.), Equation (7) yields  $\dot{r}_0/\omega_0 \cong 1.5$  m. Therefore, from Equation (4), the



variation in the radius  $r$  has an amplitude of the order of 150 cm which is within the range of laser measurements.

## CONCLUSIONS

Laser range observations of TIMATION III could provide valuable new data for the determination of various parameters associated with the dynamics of the earth. However, the successful determination of these parameters will require a very careful consideration of all perturbing forces acting on the satellite as well as information on the reflective properties and accurate dimensions of the spacecraft. By considering sets of data taken during periods of total sunlight, and by taking account of the spacecraft attitude it will be possible to compute the effects of the solar radiation force with an accuracy of at least 95%. The remaining 5% effect could amount to 25 meters along track after 10 days but will appear secular for this period and can be removed by a scale parameter. The long period lunar and solar perturbations of the orbit amount to several kilometers, but they can be computed to an accuracy of 10 centimeters for orbital arcs of one or two weeks. The satellite position uncertainty, determined by error analysis, is expected to be of the order of 1 meter with the main periodicity comparable to the orbital period of the satellite. This study indicates that polar motion, sea floor spreading, continental drift, and solid earth tides should be observable at the ten centimeter level with TIMATION III and that it could prove to be a very valuable geodynamic mission.

## ACKNOWLEDGMENT

This document is a report on a study made by members of the Geodynamics Branch.

## REFERENCE

Schindler, G. M., "Satellite Librations in the Vicinity of Equilibrium Solutions" *Astronautica ACTA*, 1959-1960.